Identifying Two-Reset Conditions for Closed-Loop Sinusoidal Input Reset Control Systems

Zhang, Xinxin; HosseinNia, S. Hassan

DOI
10.1109/MESA61532.2024.10704897

Publication date
2024

Document Version
Final published version

Published in
Proceedings of the 20th International Conference on Mechatronic, Embedded Systems and Applications, MESA 2024

Citation (APA)
Zhang, X., & HosseinNia, S. H. (2024). Identifying Two-Reset Conditions for Closed-Loop Sinusoidal Input Reset Control Systems. In *Proceedings of the 20th International Conference on Mechatronic, Embedded Systems and Applications, MESA 2024* IEEE. https://doi.org/10.1109/MESA61532.2024.10704897

2024 20th IEEE/ASME International Conference on Mechatronic and Embedded Systems and Applications (MESA) | 979-8-3315-1623-9/24/$31.00 ©2024 IEEE | DOI: 10.1109/MESA61532.2024.10704897

Identifying Two-Reset Conditions for Closed-Loop Sinusoidal Input Reset Control Systems

Xinxin Zhang
dept. Precision and Microsystems Engineering (PME)
Delft University of Technology
Mekelweg 2, Delft, NL
X.Zhang-15@tudelft.nl (0000-0003-4656-3338)

S. Hassan HosseinNia
dept. Precision and Microsystems Engineering (PME)
Delft University of Technology
Mekelweg 2, Delft, NL
S.H.HosseinNiaKani@tudelft.nl (0000-0002-7475-4628)

***Abstract*—The frequency response describes the steady-state behavior of a control system to sinusoidal inputs across varying frequencies and serves as an effective tool for system design. In closed-loop reset control systems, frequency response analysis reveals two distinct scenarios: systems with two reset instants per steady-state cycle and systems with multiple (more than two) reset instants per cycle. Existing frequency response analyses often assume only two reset instants, which can result in inaccuracies for systems with multiple resets. Additionally, multiple resets can generate high-magnitude higher-order harmonics, which may result in system performance degradation. This study introduces a novel method to identify conditions where only two reset instants occur in closed-loop reset systems. This method allows designers to avoid multiple-reset actions during the system design phase. By ensuring the system operates with only two resets per cycle, this method enhances the accuracy of frequency response analyses that assume this condition. The effectiveness of the proposed method is validated through simulations and experimental tests on a precision motion system.**

***Index Terms*—Reset control systems, frequency domain analysis, sinusoidal inputs, two resets, multiple resets, precision motion system**

I. Introduction

Reset controllers have shown their abilities in enhancing precision and speed performance in precision mechatronics industries. Pioneering this approach, the Clegg Integrator (CI) was introduced in 1958 [1]. The CI integrates a linear integrator with a reset mechanism, resetting its output to zero whenever the input signal crosses zero. Notably, the first-order harmonic of the CI displays a phase lag of 38.1 degrees, differing from the 90-degree phase lag of a linear integrator. This phase lead behavior of the CI showcases its capability to circumvent conventional Bode gain-phase limitations in linear systems [2]. Following this, several more reset controllers have been introduced, showcasing their superior capabilities compared to linear controllers, see [3]–[10].

Frequency response analysis evaluates how a system responds to sinusoidal inputs at different frequencies, capturing both phase and magnitude information, and is crucial in control system design [11]. In closed-loop reset control systems, the frequency response to periodic sinusoidal inputs can manifest in two distinct scenarios: systems featuring two reset instants per cycle, termed as "two-reset" systems, and those with more than two reset instances per cycle, termed as "multiple-reset" systems. These scenarios have distinct effects on the system's behavior and require different analysis approaches for accurate characterization.

However, prevailing frequency response analysis methods for reset systems often assume two reset instants per cycle [12]–[14], leading to inaccuracies when multiple reset instances occur. In practical applications, it is preferable to design reset control systems without multiple reset instances, as multiple resets may lead to high-magnitude higher-order harmonics. Therefore, there is a need for a tool capable of identifying the occurrence of multiple resets. Using Simulink in the time domain to identify multiple-reset systems is an option, but this approach can be inefficient and time-consuming, especially when testing across various input frequencies.

To address this gap, we introduce a novel frequency-domain method designed to identify regions of multiple-reset and two-reset occurrences in closed-loop systems. The primary contributions of this study are summarized as follows:

1) First, we propose an analysis model to decompose the steady-state responses of single-reset state Single-Input Single-Output (SISO) reset control systems under periodic sinusoidal reference inputs into piece-wise functions separated by the reset instants. Each function is calculated based on linear-time-invariant (LTI) transfer functions.
2) Then, leveraging this model, we develop a criteria for identifying regions where two-reset and multiple-reset instances occur in SISO reset control systems subjected to sinusoidal inputs.

The structure of the paper consists of six sections. Section II provides background information on reset control systems. Section III presents the research problem. Sections IV introduces two main contributions: (1) a piece-wise analysis model for closed-loop reset control systems and (2) a frequency-domain method to identify two-reset and multiple-reset systems. In Section V, the introduced technique is validated through simulations and experimental evaluations on a motion stage with three reset control systems. Finally, Section VI summarizes the results and outlines future work.

II. Preliminaries

A. The Reset Control Systems

Figure 1 displays the block diagram of a closed-loop reset control system, where $r(t)$, $e(t)$, $u(t)$, and $y(t)$ are the reference input, error, control input, and system output signals respectively. This system is comprised of a reset controller $\mathcal{C}(s)(s = j\omega)$, a linear controller $\mathcal{C}_2(s)$, and a plant $\mathcal{P}(s)$.

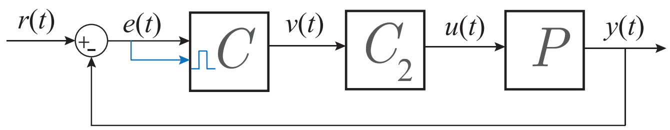

Fig. 1: The block diagram of the reset control system, where the blue lines represent the reset action.

The reset controller $\mathcal{C}(s)$ is a LTI system integrated with a reset mechanism [15], [16]. The state-space representations for a reset controller with the traditional reset mechanism, known as the "zero-crossing law" [15], are described as follows:

$$\mathcal{C} = \begin{cases} \dot{x}_r(t) = A_R x_r(t) + B_R e(t), & t \notin J, \\ x_r(t^+) = A_\rho x_r(t), & t \in J, \\ v(t) = C_R x_r(t) + D_R e(t), \end{cases} \tag{1}$$

where $x_r(t) \in \mathbb{R}^{n_c}$ denotes the state of the reset controller. The matrices A_R, B_R, C_R, and D_R are the state-space matrices of the base linear controller (BLC) of the reset controller $\mathcal{C}$, defined as

$$C_{bl}(\omega) = C_R(j\omega I - A_R)^{-1} B_R + D_R. \tag{2}$$

The second equation in (1) describes the impulsive change of the state $(x_c(t) \to x_c(t^+))$ applied whenever $t \in J$. Here, J represents the set of reset instants for $\mathcal{C}$. According to the "zero-crossing law," the reset instant, denoted as t_i, occurs when the reset-triggered signal $e(t)$ crosses zero, i.e., $e(t_i) = 0$. Therefore, J is defined as $J := \{t_i | e(t_i) = 0,\ i \in \mathbb{Z}^+\}$. When $t \in J$, the state $x_c(t)$ of $\mathcal{C}$ resets to a predetermined value determined by the reset matrix A_ρ, defined as follows:

$$A_\rho = \begin{bmatrix} A_{\rho\gamma} & \\ & I_{n_l} \end{bmatrix}, A_{\rho\gamma} = \text{diag}(\gamma_1, \gamma_2, \cdots, \gamma_o, \cdots, \gamma_{n_r}). \tag{3}$$

In (3), $\gamma_o,\ o \in \mathbb{Z}^+$ takes values in the range of $(-1, 1]$. Here, n_r represents the number of reset states, while n_l for I_{n_l} denotes the number of linear states. The number of states of $\mathcal{C}$ is expressed as $n_c = n_r + n_l$. When $n_r = 0$, the reset controller $\mathcal{C}$ is identical to the BLC $\mathcal{C}_{bl}$ (2). The reset controllers considered in this study have a single reset state, where $n_r = 1$. The reset controllers with a single reset state include common examples such as the Clegg Integrator (CI), the First-order Reset Element (FORE). [3], [4], and the Second-order Reset Element (SORE) with resetting the first state [5].

B. Frequency Responses Analysis for the Closed-loop Reset Control System

Frequency response analysis relies on system stability and convergence. While our main focus is not on those aspects, to ensure the feasibility of frequency response analysis in the proof for the main contribution, we introduce Assumption 1 to guarantee system stability [17] and convergence [18]. Additionally, the stability and convergence of reset systems can be ensured through thorough design practices.

Assumption 1. The closed-loop reset control system is assumed to be $\mathscr{L}_2$-stable, the initial condition of the reset controller $\mathcal{C}$ is zero, there are infinitely many reset instants t_i with $\lim_{t_i \to \infty} = \infty$, the input signals are Bohl functions [19], and there is no Zenoness behaviour.

Consider a SISO reset control system in Fig. 1, subjected to a reference input signal $r(t) = |R|\sin(\omega t)$, and under Assumption 1. The sensitivity function $\mathcal{S}_{DF}(\omega)$ is defined as the ratio of the Fourier transform of the steady-state error determined by describing function (DF) analysis, denoted as $E_{DF}(\omega)$, to the Fourier transform of the reference input signal, denoted as $R(\omega)$ [12], given by

$$\mathcal{S}_{DF}(\omega) = E_{DF}/(\omega)R(\omega) = 1/[1 + H_1(\omega)\mathcal{C}_2(\omega)\mathcal{P}(\omega)], \tag{4}$$

where

$$\begin{aligned} \Theta_D(\omega) &= -2\omega^2 \Delta(\omega)[\Gamma_r(\omega) - \Lambda^{-1}(\omega)]/\pi, \\ \Delta(\omega) &= I + e^{(\frac{\pi}{\omega} A_R)},\ \Delta_r(\omega) = I + A_\rho e^{(\frac{\pi}{\omega} A_R)}, \\ H_1(\omega) &= C_R(j\omega I - A_R)^{-1}(I + j\Theta_D(\omega))B_R + D_R, \\ \Lambda(\omega) &= \omega^2 I + {A_R}^2,\ \Gamma_r(\omega) = \Delta_r^{-1}(\omega) A_\rho \Delta(\omega) \Lambda^{-1}(\omega). \end{aligned} \tag{5}$$

The steady-state error of the closed-loop reset system with an input $r(t) = |R|\sin(\omega t)$, from the DF analysis (4), is given by

$$e_{DF}(t) = |R\mathcal{S}_{DF}(\omega)|\sin(\omega t + \angle \mathcal{S}_{DF}(\omega)). \tag{6}$$

C. Precision Positioning Setup

Figure 2 shows the plant used in this paper. It is a precision positioning stage with 3 degrees of freedom, called "Spyder". Three masses (M_1, M_2, M_3) are driven by three voice coil actuators (A_1, A_2, A_3) and employ a linear current source power amplifier. These masses utilize dual leaf flexures for exclusive connection to the base (M_c). Control systems are conducted on an NI compactRIO. The Mercury M2000 linear encoder ("Enc") sampled at 10 kHz and with 100 nm resolution senses mass positions. For this SISO study, only actuator A_1 positions mass M_1.

Figure 2(b) shows the Frequency Response Function (FRF) of the setup, resembling a collocated double mass-spring-damper system with additional high-frequency parasitic dynamics. The "Spyder" system's transfer function in (7) is approximated as a single eigenmode mass-spring-damper model using Matlab's identification tool for control clarity.

$$\mathcal{P}(s) = \frac{6.615e5}{83.57s^2 + 279.4s + 5.837e5}. \tag{7}$$

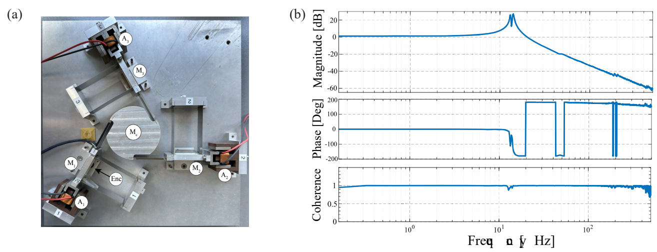

Fig. 2: (a) The planar precision positioning system "Spyder". (b) The FRF data from actuator A_1 to attached mass M_1.

III. Problem Statement

A. The Proportional-Clegg Integrator-Derivative (PCID) Control System

Figure 3 depicts the configuration of the Proportional-Clegg Integrator-Derivative (PCID) controller. This controller is constructed by substituting the integrator component in the traditional PID controller with the CI, providing additional phase lead compared to the standard PID controller. The transfer function of $\mathcal{P}(s)$ is given in (7).

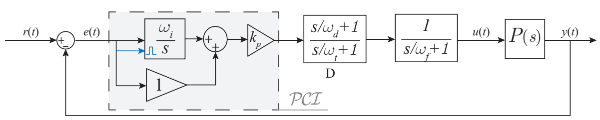

Fig. 3: The block diagram of the PCID control system.

B. Problem Statement

Figure 4 presents the steady-state error signals $e(t)$ of the PCID reset control system, specified by the parameters in C_1 of Table I, under a sinusoidal reference input $r(t) = \sin(2\pi f t)$ at input frequencies $f = 5$ Hz and $f = 100$ Hz. At $f = 5$ Hz, the PCID system exhibits characteristics of a "multiple-reset" system, while at $f = 100$ Hz, it behaves as a "two-reset" system. Current frequency response analysis and design methods for closed-loop reset control systems are built upon the assumption of a two-reset system. However, as depicted in Fig. 4(a), this assumption is not always assured.

Consider a SISO reset control system in Fig. 1 with the reference signal $r(t) = \sin(2\pi f t)$. The Root Mean Square (RMS) values of the steady state error signal $e(t)$ obtained from simulation and DF analysis (6) are denoted as $||e||_2^{\text{Sim}}$ and $||e||_2^{\text{DF}}$, respectively. In Fig. 5, when dealing with multiple-reset systems shaded in grey, the classical DF fails to provide accurate analysis of the system's behaviour.

Therefore, the research aims to propose a method that distinguishes between multiple-reset and two-reset systems, ensuring the accuracy of frequency response analysis and aiding in avoiding multiple resets. The research problem can be described as follows:

Consider a SISO reset control system as shown in Fig. 1, with the reference signal $r(t) = |R|\sin(\omega t)$, where $\omega \in \mathbb{R}^+$, at steady states and under Assumption 1. The research problem

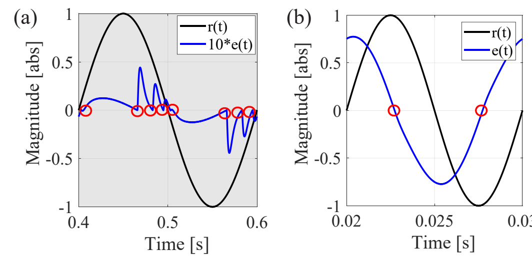

Fig. 4: The steady state error signal $e(t)$ (in blue) and the input signal $r(t)$ (in black) in a PCID control system in closed-loop under two input frequencies, (a) $f = 5$ Hz (in grey background) and (b) $f = 100$ Hz (in white background), respectively. The red circles mark the reset instants per cycle.

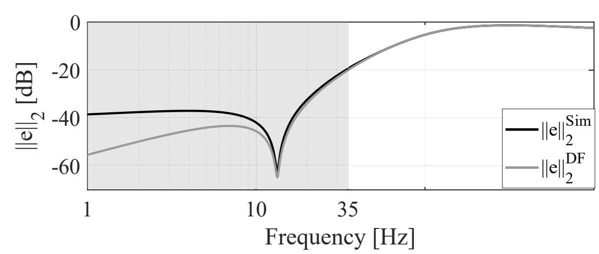

Fig. 5: The RMS of the steady state error $e(t)$ obtained from simulation $||e||_2^{\text{Sim}}$ and the DF analysis $||e||_2^{\text{DF}}$.

is to develop a method for identifying the frequency ranges associated with two-reset and multiple-reset systems. The proposed method should take as input the transfer functions $\mathcal{C}(s)$, $\mathcal{C}_2(s)$, and $\mathcal{P}(s)$ of the reset control system and the input frequency ω, and provide as output whether the system exhibits multiple-reset or two-reset behavior.

IV. Identifying the Two-reset and the Multiple-reset Systems

This section introduces the frequency-domain-based method for identifying multiple-reset and two-reset systems as presented in Theorem 1.

Define the base-linear system (BLS) of the reset system depicted in Fig. 1 by replacing the reset controller $\mathcal{C}$ with its Base-Linear Controller (BLC) $\mathcal{C}_{bl}$ (2). Consider the BLS under a sinusoidal reference input signal $r(t) = |R|\sin(\omega t)$, where ω is the input frequency, and its Fourier transform is denoted as $R(\omega)$. Let $e_{bl}(t)$ be the steady-state error of the BLS, with Fourier transforms denoted as $E_{bl}(\omega)$. The base-linear sensitivity function is defined as:

$$\mathcal{S}_{bl}(\omega) = \frac{E_{bl}(\omega)}{R(\omega)} = \frac{1}{1 + \mathcal{C}_{bl}(\omega)\mathcal{C}_2(\omega)\mathcal{P}(\omega)}. \tag{8}$$

Then, the base-linear steady-state error $e_{bl}(t)$ is given by

$$e_{bl}(t) = |\mathcal{S}_{bl}(\omega)|\sin(\omega t + \angle\mathcal{S}_{bl}(\omega)),\ \angle\mathcal{S}_{bl}(\omega) \in (-\pi,\ \pi]. \tag{9}$$

During one steady-state cycle, the first zero-crossing point of the base-linear system is given by

$$t_1 = \begin{cases} (\pi - \angle \mathcal{S}_{bl}(\omega))/\omega, & \text{for } \angle \mathcal{S}_{bl}(\omega) \in (0,\ \pi], \\ (-\angle \mathcal{S}_{bl}(\omega))/\omega, & \text{for } \angle \mathcal{S}_{bl}(\omega) \in (-\pi,\ 0]. \end{cases} \tag{10}$$

The closed-loop reset control system shown in Fig. 1, with a sinusoidal input signal $r(t) = |R|\sin(\omega t)$, and under Assumption 1, undergoes transient responses before reaching steady state. The reset action during the transient response phase may influence the subsequent steady-state behavior. However, transient responses are typically minimized in the system design. The starting time of one steady-state cycle, denoted by t_0, is defined as the instant when $r(t_0) = 0$ and $\dot{r}(t_0) > 0$. We assume the impact of reset actions during transients on steady-state responses is negligible by making the following assumption:

Assumption 2. The closed-loop reset system under a sinusoidal reference input signal $r(t) = |R|\sin(\omega t)$ at steady states, satisfying Assumption 1, behaves the same as its BLS before the time instant t_1 given in (10).

The following theorem presents a method for identifying two-reset actions in closed-loop reset systems under sinusoidal inputs at steady states.

Theorem 1. (Two-Reset Conditions for Closed-Loop Reset Systems) Consider a closed-loop reset control system (as shown in Fig. 1) with a sinusoidal reference input $r(t) = |R|\sin(\omega t)$. Under Assumptions 1 and 2, the system is identified as a two-reset system if, for all $t_\delta \in (0, t_m)$, the following condition holds:

$$\Delta(\omega, t_\delta) = -|\mathcal{S}_{bl}(\omega)|\sin(\omega t_\delta) + h_\alpha(t_\delta)|\Theta_{bl}(\omega)|\sin(\angle \Phi_{bl}(\omega)) < 0, \tag{11}$$

where

$$\begin{aligned} \Theta_{bl}(\omega) &= \Phi_{bl}(\omega)\mathcal{S}_{bl}(\omega), \\ \Phi_{bl}(\omega) &= (j\omega I - A_R)^{-1}B_R, \\ \mathcal{T}_\alpha(\omega) &= \mathcal{C}_2(\omega)\mathcal{P}(\omega)\mathcal{S}_{bl}(\omega), \\ \Delta_x(\omega) &= C_R(j\omega I - A_R)^{-1}j\omega I, \\ h_\alpha(t) &= \mathscr{F}^{-1}[(A_\rho - I)H(\omega)\mathcal{T}_\alpha(\omega)\Delta_x(\omega)], \\ H(\omega) &= \mathscr{F}[h(t)] = 1/(j\omega),\ h(t) := \begin{cases} 1, & t > 0, \\ 0, & t \leq 0, \end{cases} \\ t_m &= \begin{cases} \angle \mathcal{S}_{bl}(\omega)/\omega, & \text{for } \angle \mathcal{S}_{bl}(\omega) \in (0,\ \pi], \\ (\pi + \angle \mathcal{S}_{bl}(\omega))/\omega, & \text{for } \angle \mathcal{S}_{bl}(\omega) \in (-\pi,\ 0]. \end{cases} \end{aligned} \tag{12}$$

Proof. The proof is provided in Appendix. A. □

V. Illustrative Examples

A. The PCID Control Systems Design

We design three PCID control systems (in Fig. 3), denoted as C_1-C_3, as illustrative examples. The parameters for these systems are outlined in Table I, where $\omega_i = 2\pi f_i$, $\omega_c = 2\pi f_c$, $\omega_d = 2\pi f_d$, and $\omega_t = 2\pi f_t$, $\omega_f = 10\omega_c$.

TABLE I: Parameters of systems $\mathcal{C}_1$, $\mathcal{C}_2$, and $\mathcal{C}_3$, where γ is the reset value and $\mathbf{f_b}$ is defined in Definition 1.

PCID	BW(Hz)	Phase(°)	f_i(Hz)	f_d(Hz)	f_t(Hz)	γ	kp	$\mathbf{f_b}$(Hz)
$\mathcal{C}_1$	150	60	15	25.4	885.9	0	15.1	**35**
$\mathcal{C}_2$	150	60	15	24.6	913.1	0.8	18.0	**18**
$\mathcal{C}_3$	200	60	20	34.3	1164.5	-0.2	28.7	**52**

B. Experimental Validation for Theorem 1

Definition 1. The frequency f_b satisfying $\Delta(f_b) = 0$ determined by (11) is defined as the boundary frequency that distinguishes between the two-reset and multiple-reset systems.

The boundary frequencies (f_b) for control systems $\mathcal{C}_1$, $\mathcal{C}_2$, and $\mathcal{C}_3$, determined by Theorem 1, are 35 Hz, 18 Hz, and 52 Hz, respectively, as listed in Table I. In Fig. 6, we measured the steady state error signal $e(t)$ and reference input signal $r(t) = \sin(2\pi f t)$ for input frequencies $f = f_b$ Hz and $f = f_b \pm 10$ Hz in the three control systems through experiments. Results show that, at the predicted boundary frequency f_b, there exist 3-4 reset instants during each steady state cycle. Lower frequencies exhibit more reset instants (shaed in grey), while higher frequencies display 2 reset instants. These results confirm f_b as the threshold frequency, separating the two-reset and multiple-reset regions, thus validating Theorem 1. Note that the jagged signals in Fig. 6(a_2) and 6(b_2) may result from external base disturbances.

C. The Usability and Limitation of Theorem 1

The RMS of the steady state errors $||e||_2$ of system $\mathcal{C}_1$, as well as systems $\mathcal{C}_2$ and $\mathcal{C}_3$ is shown in Fig. 5 and Fig. 7. The boundary frequency f_b effectively distinguishes between two regions: multiple-reset systems shaded in grey, and two-reset systems shaded in white.

In multiple-reset systems, the prediction error of the DF is notably larger compared to two-reset systems. This underscores the effectiveness of employing the Theorem 1 to identify regions where the closed-loop analysis maintains its accuracy. In system C_3, in two-reset systems shaded in white, there exists a discrepancy between the DF analysis and the simulation results. This occurs because the DF analysis only considers the first-order harmonic of the error signal, but in reality there are infinite harmonics present in the closed-loop reset system. However, to develop more precise frequency response analysis is not the paper's focus. Given that existing response analysis methods [12]–[14] typically assume two-reset systems, our method enables the identification of two-reset systems, facilitating more accurate predictions through frequency response analysis. Nevertheless, the effectiveness of this method is limited by Assumption 2. For a system with poor transient response that Assumption 2 is not satisfied, the method may lose accuracy.

VI. Conclusion

This study presents a novel frequency-domain method for identifying two-reset systems with sinusoidal inputs. Exper-

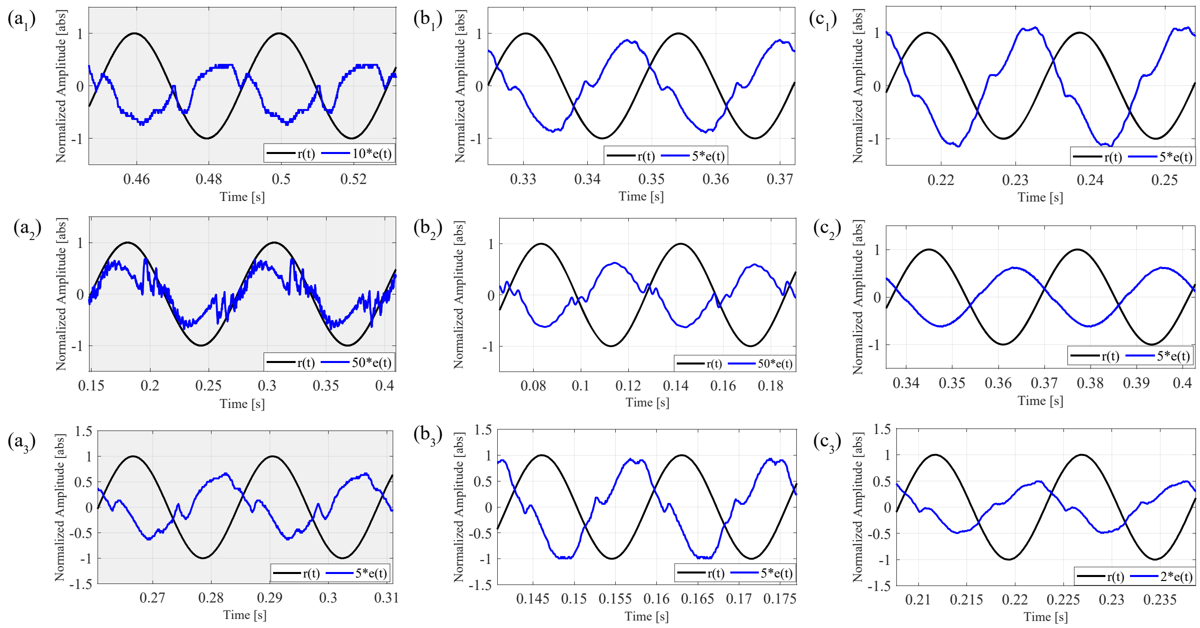

Fig. 6: Measured steady state errors $e(t)$ and reference inputs $r(t)$ for system $\mathcal{C}_1$ at input frequencies f of (a_1) 25 Hz, (b_1) 35 Hz, and (c_1) 45 Hz. For system $\mathcal{C}_2$, the input frequencies are (a_2) 8 Hz, (v_2) 18 Hz, and (c_2) 28 Hz. For system $\mathcal{C}_3$, at input frequencies (a_3) 42 Hz, (b_3) 52 Hz, and (c_3) 62 Hz. The grey background indicates the multiple-reset systems.

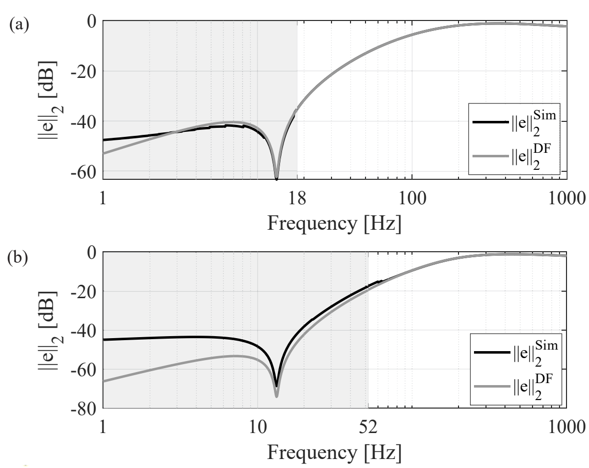

Fig. 7: The $||e||_2$ for (a) system $\mathcal{C}_2$ and (b) system $\mathcal{C}_3$.

imental validation on a motion stage confirms the method's efficacy. Frequency response analysis is a crucial tool for system design, but current approaches for closed-loop reset systems often assume a two-reset scenario, leading to inaccuracies in systems with multiple resets. Moreover, multiple-reset actions can introduce redundant higher-order harmonics and degrade system performance. The proposed method helps avoid multiple-reset actions during system design, ensuring accurate frequency response analysis for reset systems. Future research may further enhance the practical applicability of this method in engineering applications.

References

[1] John C Clegg. A nonlinear integrator for servomechanisms. *Transactions of the American Institute of Electrical Engineers, Part II: Applications and Industry*, 77(1):41–42, 1958.

[2] Linda Chen, Niranjan Saikumar, Simone Baldi, and S Hassan HosseinNia. Beyond the waterbed effect: Development of fractional order crone control with non-linear reset. In *2018 annual american control conference (ACC)*, pages 545–552. IEEE, 2018.

[3] Isaac Horowitz and Patrick Rosenbaum. Non-linear design for cost of feedback reduction in systems with large parameter uncertainty. *International Journal of Control*, 21(6):977–1001, 1975.

[4] KR Krishnan and IM Horowitz. Synthesis of a non-linear feedback system with significant plant-ignorance for prescribed system tolerances. *International Journal of Control*, 19(4):689–706, 1974.

[5] Leroy Hazeleger, Marcel Heertjes, and Henk Nijmeijer. Second-order reset elements for stage control design. In *2016 American Control Conference (ACC)*, pages 2643–2648. IEEE, 2016.

[6] Niranjan Saikumar, Rahul Kumar Sinha, and S Hassan HosseinNia. "constant in gain lead in phase" element–application in precision motion control. *IEEE/ASME Transactions on Mechatronics*, 24(3):1176–1185, 2019.

[7] Niranjan Saikumar and Hassan HosseinNia. Generalized fractional order reset element (gfrore). In *9th European Nonlinear Dynamics Conference (ENOC)*, 2017.

[8] Christoph Weise, Kai Wulff, and Johann Reger. Fractional-order memory reset control for integer-order lti systems. In *2019 IEEE 58th conference on decision and control (CDC)*, pages 5710–5715. IEEE, 2019.

[9] Alfonso Baños and Angel Vidal. Definition and tuning of a pi+ ci reset controller. In *2007 european control conference (ECC)*, pages 4792–4798. IEEE, 2007.

[10] DA Deenen, Marcel François Heertjes, WPMH Heemels, and Henk Nijmeijer. Hybrid integrator design for enhanced tracking in motion control. In *2017 American Control Conference (ACC)*, pages 2863–2868. IEEE, 2017.

[11] Sigurd Skogestad and Ian Postlethwaite. *Multivariable feedback control: analysis and design*. john Wiley & sons, 2005.

[12] Yuqian Guo, Youyi Wang, and Lihua Xie. Frequency-domain properties of reset systems with application in hard-disk-drive systems. *IEEE Transactions on Control Systems Technology*, 17(6):1446–1453, 2009.

[13] Niranjan Saikumar, Kars Heinen, and S Hassan HosseinNia. Loop-shaping for reset control systems: A higher-order sinusoidal-input describing functions approach. *Control Engineering Practice*, 111:104808, 2021.
[14] Xinxin Zhang, Marcin B Kaczmarek, and S Hassan HosseinNia. Frequency-domain analysis for reset systems using pulse-based model. *arXiv preprint arXiv:2206.00523*, 2022.
[15] Alfonso Banos and Antonio Barreiro. *Reset control systems*. Springer, 2012.
[16] Yuqian Guo and Yanying Chen. Stability analysis of delayed reset systems with distributed state resetting. *Nonlinear Analysis: Hybrid Systems*, 31:265–274, 2019.
[17] Orhan Beker, CV Hollot, Yossi Chait, and Huaizhong Han. Fundamental properties of reset control systems. *Automatica*, 40(6):905–915, 2004.
[18] Ali Ahmadi Dastjerdi, Alessandro Astolfi, and S Hassan HosseinNia. A frequency-domain stability method for reset systems. In *2020 59th IEEE Conference on Decision and Control (CDC)*, pages 5785–5791. IEEE, 2020.
[19] EA Barabanov and AV Konyukh. Bohl exponents of linear differential systems. *Mem. Differential Equations Math. Phys*, 24:151–158, 2001.
[20] Xinxin Zhang and S. Hassan HosseinNia. Frequency-domain analysis for infinite resets systems*. In *2023 IEEE International Conference on Mechatronics (ICM)*, pages 1–6, 2023.

APPENDIX

A. The Proof for Theorem 1

Proof. Under Assumption 1, the reset system (in Fig. 1) with a sinusoidal reference input $r(t) = |R|\sin(\omega t)$ has the steady-state period of $2\pi/\omega$. The reset instant $t_i \in J$ satisfies the criterion $e(t_i) = r(t_i) - y(t_i) = 0$.

From literature [20], the steady-state error signal of a closed-loop reset system under sinusoidal inputs is a piece-wise function, with each piece determined by the reset instants $t_i \in J$. The second piece-wise steady-state error $e_2(t)$ during the time interval $[t_1, t_2)$ is as follows:

$$e_2(t) = e_{bl}(t) - x_{bl}(t_1)h_\alpha(t - t_1), \tag{13}$$

where $h_\alpha(t - t_1)$ defined in (12) is a step response.

In a closed-loop reset control system with a sinusoidal reference input $r(t) = |R|\sin(\omega t)$, under Assumption 1, multiple-reset systems are defined as systems where the error signal $e(t)$ resets more than twice per cycle during steady states. The condition for a multiple-reset scenario in a reset control system is equivalent to the existence of solutions to $e_2(t) = 0$ in (13) for $t \in (t_1, \pi/\omega)$. Define

$$e_{2nl}(t) = -x_{bl}(t_1)h_\alpha(t - t_1), \tag{14}$$

and substitute $e_{2nl}(t)$ into (13), $e_2(t)$ in (13) is given by

$$e_2(t) = e_{bl}(t) + e_{2nl}(t). \tag{15}$$

Define $t^* = t - t_1$ and substitute t^* into (14), $e_{2nl}(t^*)$ is expressed as

$$e_{2nl}(t^*) = -x_{bl}(t_1)h_\alpha(t^*). \tag{16}$$

Since the closed-loop reset system is convergent and stable under Assumption 1, and $e_{2nl}(t^*)$ is a step response as defined in (16), it has a unilateral Laplace transform in continuous time. From (12), the Laplace transform of $e_{2nl}(t^*)$, denoted by $E_{2nl}(s), s = j\omega$, is given by:

$$E_{2nl}(s) = -x_{bl}(t_1)(A_\rho - I)H(s)\Phi_{bl}(s)\mathcal{T}_\alpha(s). \tag{17}$$

From (17) and based on the Final Value Theorem, the steady-state value of $e_{2nl}(t^*)$ in (16) is given by:

$$\lim_{t^* \to \infty} e_{2nl}(t^*) = \lim_{s \to 0} sE_{2nl}(s) = 0. \tag{18}$$

Equation (18) indicates that $e_{2nl}(t^*)$ asymptotically converges to zero. From (15) and (18), we have

$$\lim_{t^* \to \infty} e_2(t^*) = e_{bl}(t). \tag{19}$$

Equation (19) indicates $e_2(t^*)$ asymptotically converges to $e_{bl}(t)$ over time.

From (9) and (10), during the time interval $(t_1, \pi/\omega)$, we have

$$\begin{cases} \dot{e}_{bl}(t_1) < 0, & \text{for } \angle\mathcal{S}_{bl}(\omega) \in (0,\ \pi], \\ \dot{e}_{bl}(t_1) > 0, & \text{for } \angle\mathcal{S}_{bl}(\omega) \in (-\pi,\ 0] \end{cases} \tag{20}$$

When $\angle\mathcal{S}_{bl}(\omega) \in (0,\ \pi]$, from (9), we have:

$$e_{bl}(t) = |R||\mathcal{S}_{bl}(\omega)|\sin(\omega t + \angle\mathcal{S}_{bl}(\omega)) < 0,\ \text{for } t \in (t_1, \pi/\omega). \tag{21}$$

The sufficient condition for multiple-reset occurrence is that there exists a solution for

$$\max_{t \in (t_1, \pi/\omega)} e_2(t) \geq 0. \tag{22}$$

Define $t' = t - t_1$. From (13), $e_2(t)$ is given by

$$e_2(t) = -|R||\mathcal{S}_{bl}(\omega)|\sin(\omega t') - h_\alpha(t - t_1)x_{bl}(t_1). \tag{23}$$

From (9) and (10), $x_{bl}(t_1)$ is given by

$$x_{bl}(t_1) = -|R||\Theta_{bl}(\omega)|\sin(\angle\Phi_{bl}(\omega)). \tag{24}$$

Substituting $x_{bl}(t_1)$ from (24) into (23), we have:

$$e_2(t) = -|R||\mathcal{S}_{bl}(\omega)|\sin(\omega t') + h_\alpha(t')|R||\Theta_{bl}(\omega)|\sin(\angle\Phi_{bl}(\omega)). \tag{25}$$

From (22), the sufficient condition for the existence of the multiple-reset system is:

$$\max_{t' \in (0, \pi/\omega - t_1)} e_2(t) \geq 0. \tag{26}$$

Define $\Delta(\omega, t_\delta) = e_2(t)/|R|$. From (25) and (26), the sufficient condition for the existence of a multiple-reset system is that there exists a time instant $t_\delta \in (0, \pi/\omega - t_1)$, such that:

$$\Delta(\omega, t_\delta) = -|\mathcal{S}_{bl}(\omega)|\sin(\omega t') + h_\alpha(t')|\Theta_{bl}(\omega)|\sin(\angle\Phi_{bl}(\omega)) \geq 0. \tag{27}$$

From (21), during the time interval $(0, \pi/\omega - t_1)$, $e_{bl}(t) < 0$. Thus, from (27), the multiple-reset systems require $\Delta(\omega, t_\delta) \geq 0$ has solution.

For scenarios where $\angle\mathcal{S}_{bl}(\omega) \in (-\pi, 0]$, the condition for multiple-reset systems remains unchanged, and the derivation process for this scenario is similar to previous cases. Therefore, the detailed derivation is not repeated here.

Define $t_m = \pi/\omega$. From (10), t_m is given by

$$t_m = \begin{cases} \angle\mathcal{S}_{bl}(\omega)/\omega, & \text{for } \angle\mathcal{S}_{bl}(\omega) \in (0,\ \pi], \\ (\pi + \angle\mathcal{S}_{bl}(\omega))/\omega, & \text{for } \angle\mathcal{S}_{bl}(\omega) \in (-\pi,\ 0]. \end{cases} \tag{28}$$

Therefore, for both $\angle\mathcal{S}_{bl}(\omega) \in (-\pi, 0]$ and $\angle\mathcal{S}_{bl}(\omega) \in (0, \pi]$, the conditions for two-reset systems are met if, for all $t_\delta \in (0, t_m)$, the inequality $\Delta(\omega, t_\delta) < 0$ holds, as demonstrated in Theorem 1. This completes the proof. $\square$